Monitoring of antibody glycosylation pattern based on microarray MALDI-TOF mass spectrometry

Author(s):
Hajduk, Joanna; Wolf, Moritz; Steinhoff, Robert; Karst, Daniel; Souquet, Jonathan; Broly, Hervé; Morbidelli, Massimo; Zenobi, Renato

Publication date:
2019-08-20

Permanent link:
https://doi.org/10.3929/ethz-b-000351707

Originally published in:
Journal of Biotechnology 302, https://doi.org/10.1016/j.jbiotec.2019.06.306

Monitoring of antibody glycosylation pattern based on microarray MALDI-TOF mass spectrometry

Joanna Hajduk[a], Moritz Wolf[b], Robert Steinhoff[a], Daniel Karst[b], Jonathan Souquet[c], Hervé Broly[c], Massimo Morbidelli[b] and Renato Zenobi[a]

[a] Laboratory of Organic Chemistry, Department of Chemistry and Applied Biosciences, ETH Zurich, CH-8093 Zurich, Switzerland
[b] Institute for Chemical and Bioengineering, Department of Chemistry and Applied Biosciences, ETH Zurich, CH-8093 Zurich, Switzerland
[c] Biotech Process Science Technology & Innovation, Merck-Serono S.A., Corsier-sur-Vevey, Switzerland

Corresponding author:
Prof. Renato Zenobi
Laboratory of Organic Chemistry
Department of Chemistry and Applied Biosciences
ETH Zurich
Vladimir-Prelog-Weg 3, CH-8093 Zurich, Switzerland
Phone: +41 44 632 43 76; fax: +41 44 632 12 92; e-mail: zenobi@org.chem.ethz.ch

Abstract

Biologically manufactured monoclonal antibodies (mAb) can strongly vary in their efficacy and affinity. Therefore, engineering and production of the mAb is highly regulated and requires product monitoring, especially in terms of N-glycosylation patterns. In this work, we present a high-throughput matrix-assisted laser desorption/ionization mass spectrometry (MALDI-MS) method based on a microarray technology to monitor N-glycopeptides of IgG1 produced in a perfusion cell culture. A bottom-up approach combined with zwitterionic-hydrophilic interaction liquid chromatography for sample purification was used to determine the day-by-day variation of the terminal galactose within two major N-glycoforms. Our results show that microarrays for mass spectrometry (MAMS) are a robust platform for the rapid determination of the carbohydrate distribution. The spectral repeatability is characterized by a low coefficient of variations (1.7% and 7.1% for the FA2 and FA2G1 structures, respectively) and allows to detect the N-glycosylation variability resulting from operating conditions during the bioreactor process. The observed trend of released N-glycans was confirmed using capillary gel electrophoresis with laser-induced fluorescence detection. Therefore, the microarray technology is a promising analytical tool for glycosylation control during the production process of recombinant proteins.

Keywords: MALDI-MS, Microarray for mass spectrometry (MAMS), Monoclonal antibody, N-linked glycosylation, perfusion bioreactor

Glycosylation nomenclature

A2	$GlcNAc_2Man_3GlcNAc_2$
FA1	$GlcNAcMan_3GlcNAc_2Fuc$
FA2	$GlcNAc_2Man_3GlcNAc_2Fuc$
FA2G1	$GalGlcNAc_2Man_3GlcNAc_2Fuc$
FA2G2	$Gal_2GlcNAc_2Man_3GlcNAc_2Fuc$
M5	$Man_5GlcNAc_2$
M6	$Man_6GlcNAc_2$
M7	$Man_7GlcNAc_2$

1. Introduction

Monoclonal antibodies (mAb) have been developed from tools in fundamental biological research to diagnostic agents, and have been implemented in antibody-based therapies for over 30 years (Walsh, 2018). Especially in the oncology area, mAbs offer benefits over the traditional pharmacotherapy due to their ability to target specific antigenic epitopes, which limits adverse side effects on healthy cells. However, the excitement about their therapeutic potential is also based on the capabilities to manufacture their structure in biotechnological processes with defined specificity in virtually unlimited amounts (Hudson and Souriau, 2003).

Different manufacturing strategies (batch, fed-batch and perfusion) for cell-culture derived biopharmaceuticals contribute to overall differences in mAb quality. Particularly, N-glycosylation – present at both Cγ2 domain at asparagine (N297) position (Jefferis, 2009) is considered to be a critical quality attribute (CQA) in the Y-shaped immunoglobulin type G (IgG) and represents one of the main sources of mAb's heterogeneities with potential impact on product stability, bioactivity and safety (Reusch and Tejada, 2015). It has been suggested that the presence of Fc N-glycans contributes to proper Cγ2 domain orientation or by motion of highly dynamic N-glycan termini affects the binding affinity (Barb and Prestegard, 2011). However, recent evidence proposes their main role to be stabilization of the Cγ2 C'E loop via intermolecular interactions between carbohydrate and amino acid residues, organizing the FcγR interface for optimal binding (Nimmerjahn and Ravetch, 2008; Subedi and Barb, 2015). Ivarsson et al. (2014) demonstrated that chemical and mechanical stress parameters during manufacturing process affect the N-linked glycosylation profile. Especially, pH and dissolved oxygen tension have a profound influence, as in so-called "shift-based" experiments, significant changes of the most abundant glycoforms were observed within 28 hours. Similar effects are related to variability of cellular environment such as availability of carbon sources and nucleotide sugar donors (Wong et al., 2010) or possible differences in gene expression (Bertrand et al., 2019) throughout the entire cultivation process. In batch and fed-batch bioreactors, the cells and recombinant proteins accumulate inside the unit and are exposed to changing environmental conditions. Thus, an increasing content of toxic by-products promotes undesired chemical and enzymatic modifications. One solution to this problem is the use of perfusion bioreactors that allow cell cultivation with continuous delivery of fresh media and removal of waste products (Karst et al., 2017a; Villiger et al., 2016) and therefore offering higher productivity by maintaining stable conditions. The average perfusion duration is longer than in fed-batch setups, and this calls consequently for more monitoring points in order to exclude any potential time-dependent changes of the product.

The quality guidelines for registration of pharmaceuticals for human use require the determination of glycoproteins with respect to carbohydrate content, pattern and glycosylation site (Largy et al., 2017). Therefore, fast and simple approaches for characterizing and monitoring glycosylation are of great interest for the biopharmaceutical industry. Current strategies are clustered in top-down and bottom-up and involve analytical methods such as high-performance liquid chromatography (HPLC) (Lauber et al., 2015), capillary electrophoresis (CE) (Mittermayr et al., 2011; Reusch et al., 2014), lectin-based microarrays (Fanayan et al., 2012) and mass spectrometry (MS) (Pabst and Altmann, 2011; L. Zhang et al., 2016). Among them, MS techniques allow characterization of glycosylation at three different molecular levels, including intact proteins, glycopeptides, or released glycans (P. Zhang et al., 2016). Generally, natural carbohydrates have poor ionization efficiency and fluorescent labeling is required for sensitive detection (Ruhaak et al., 2010). Typically, the sample preparation involves multiple time-consuming experimental steps that often preclude application for daily control of a running bioprocess. Therefore, matrix-assisted laser desorption/ionization (MALDI) MS offers a unique opportunity

enabling ionization of underivatized carbohydrates and retaining the structural integrity of glycopeptides. MALDI has been identified as a promising method for rapid mAb and N-glycan analysis due to its sensitivity, high salt tolerance, and also the possibility to improve spot-to-spot inhomogeneity when using the recently introduced microarray for mass spectrometry (MAMS) technology (Steinhoff et al., 2016). With this miniaturized chip system, the irregularity of matrix crystallization and thus the frequently observed “coffee-ring" and "hot spot" effects can be reduced. Simultaneously, in combination with am automated deposition device, the total run time improves in a cost-effective way (the estimated cost is per sample is $10, including chip fabrication and consumables) making it an attractive tool for high-throughput screening analysis.

In this work, we present – to the best of our knowledge – the very first microarray-based MALDI-TOF mass spectrometric methodology for characterizing glycosylation in a biopharmaceutical process. The experiment was designed such that the N-glycan profile of a mAb can be monitored daily from a running perfusion bioreactor. The main glycoforms, which differ by a terminal galactose unit (±162 Da), are analyzed in a bottom-up approach with zwitterionic - hydrophilic interaction liquid chromatography (ZIC-HILIC). The abundance and day-by-day variations are determined based on a novel MAMS technology with MALDI-MS detection. MAMS are microstructured sample carriers with spot sizes of 400 µm, which provides minimal sample consumption and highly reproducible results. Lastly, to verify the potential of the proposed strategy in glycosylation quality control or even in-process control, results are benchmarked against capillary gel electrophoresis with laser-induced fluorescence detection (CGE-LIF) (Callewaert et al., 2004a, 2004b).

2. Materials & Methods

2.1. Materials

Millipore water (18.2 MΩ x cm) was used. LC–MS grade acetonitrile (ACN) and isopropanol were bought from Sigma-Aldrich, Switzerland. Trifluoroacetic acid (TFA) (Sigma-Aldrich, Switzerland) was used without any dilution or purification. The matrix α-cyano-4-hydroxycinnamic acid (HCCA) was purchased from Sigma-Aldrich, Switzerland. The GPEP FA2 glycopeptide standard was supplied by Ludger, United Kingdom.

2.2. Reactor operation

A proprietary Chinese hamster ovary (CHO) cell line (Merck Serono) producing an IgG1 recombinant monoclonal antibody (mAb) was thawed from liquid N_2 and passaged every two days. The cells were cultured in humid atmosphere at 36.5°C, 5% CO_2, and 320 rpm using a shaking incubator with 25 mm orbital throw (Kuhner AG, Switzerland) for one week. Cells were cultured in 50 mL shake tubes (TubeSpin®, TPP, Switzerland), and when the culture volume exceeded 100 mL, cells were cultivated in roller bottles (Corning®, USA), and the shaking speed was adjusted to 130 rpm. Then, cells were transferred into a perfused seed bioreactor for another week to reach a cell density of above $50x10^6$ cells/mL. The reactor setup employed a tangential flow filtration (TFF) system for cell retention (Karst et al., 2016). During the first four days, the harvest rate was fixed to 1 reactor volume per day, and then further increased to 2 reactor volumes per day. In a next step, cells were inoculated to a 1.5L working volume perfusion bioreactor (Vaudaux-Eppendorf, Switzerland) employing an alternated tangential flow (ATF) filtration system for cell retention (Karst et al., 2016). The overall perfusion rate was controlled at 1 reactor volume exchange rate per day (1 RV/day). The cell density was controlled at 40×10^6 cells/day during the first 10 days, and afterwards at $50x10^6$ cells/day for another 8 days by adapting the bleed rate according to an online biomass sensor (Aber Instruments Ltd., Wales).

Operating set points were 36.5°C, pH 7.1, and 50% dissolved oxygen tension. Daily samples were taken to monitor viable cell density, viability, mAb titer and glucose (Glc) as well as lactate concentrations (Lac). Glc and Lac concentration were measured using a common blood analyser (Hitado SuperGL compact, Sysmex GmbH, Germany).

2.3. HPLC-UV analysis

Antibody quantification was performed using a protein A column (Poros A-20, 2.1 mm x 30 mm) from Life Technologies (Carlsbad, CA, USA), and 20 mM phosphate, 150 mM NaCl, pH 7.5 as binding and washing solution. For the elution buffer, 10 mM HCL, 150 mM NaCl, pH 2 were used in combination with 20% acetic acid for regeneration of the column. For antibody detection, UV absorbance at 280 nm was used (Table S1 with a details about the perfusion culture conditions).

2.4. In-solution digestion and sample purification

Prior to proteolytic digestion, all supernatant samples taken from the perfusion bioreactor were purified using Vivapure miniprepA columns (Sartorius Stedim Biotech, Goettingen, Germany) and were desalted using 30 kDa cut-off spin columns (Amicon Ultra 0.5 mL centrifugal filters, Merck Millipore) as recommended by the manufacturer's protocols. Subsequently, the purified mAbs were subjected to in-solution digestion. Briefly, 50 µg of mAb was diluted with 50 mM ammonium bicarbonate and reduced with 5.6 mM dithiothreitol for 5 min at 60°C. In order to carbamidomethylate the sulfhydryl groups, the samples were alkylated with 10 mM iodoacetamide for 20 min in the dark at RT. The mAb was then digested overnight using trypsin (Sigma, cat. no. T6567) with a 1:50 enzyme-to-substrate ratio at 37°C overnight. Each sample collected within 18 days of the bioreactor process was digested in triplicate. Before MS measurement, the peptides derived from tryptic digestion were purified using ZIC®-HILIC solid phase extraction (SPE) cartridges (SeQuant, Umeå, Sweden). First, the samples were adjusted to a concentration of 50% acetonitrile. The peptides were then loaded into the SPE sorbent and washed with 100% acetonitrile. The polar compounds were eluted with 100 µL water and concentrated up to 20 µL using SpeedVac concentrator.

2.5. N-glycopeptides analysis

2.5.1. Microarray for mass spectrometry (MAMS)

N-glycopeptide profiles were monitored using MAMS targets (Pabst et al., 2013). The MAMS chip was manufactured from ITO coated glass slides (75 mm×25 mm, sheet resistance 15−25Ω/sq) (Sigma-Aldrich, Buchs, Switzerland) and coated with polysilazane (CAG37, Clariant, Muttenz, Switzerland). The chip's microarray pattern consists of 8 columns that each contains one large reservoir spot (inner diameter of 1 mm, depth of 30−50µm) positioned at the top and followed by 12 small spots (inner diameter of 400 µm, gap distance 500−750 µm). All of these spots were created by laser ablation, using a Nd:YAG laser (SuperRapid from Lumera Laser, Kaiserslautern, Germany). The laser beam was focused and scanned over the surface of the sample using a galvanoscanner (hurrySCAN 10 from Scanlab, Puchheim/Munich, Germany). A telecentric lens with a 100 mm working distance delivered a constant focal spot of ~10µm at the surface over the scanned area. The scan speed (150 mm s^{-1}) and the hatch were selected to have a 3 µm spot-to-spot distance.

2.5.2. MALDI-MS analysis

To create homogenous analyte-matrix spots for MALDI-MS, 1 µL of peptide solution was deposited onto the reservoir spot of MAMS's chip. The droplet was then dragged across the pattern array using an automated metal sliding device, which generated up to 12 technical replicates. After the analyte

droplets had dried, the 1 µL of matrix solution (5 mg/mL HCCA in 50% acetonitrile, 0.1% TFA) was deposited in the reservoir spot and distributed in the same manner to coat the analyte molecules. N-glycopeptide analysis was performed on a ABSciex 5800 MALDI-TOF/TOF mass spectrometer using MAMS plates. The instrument is equipped with a laser system with a maximum repetition rate of 1 kHz. The spectra were recorded in positive-ion reflectron mode with a laser intensity of 3500 – 4000 [arb. units] and 15 sub-spectra on 30 different positions were acquired per spot. Spectra were analysed over a mass range from 700 – 4000 Da. The source voltage was 15 kV. For the external calibration of the mass spectrometer, a peptide calibration Mix4 (Proteomix, Laserbio Labs) was used. The N-glycopeptides were identified using a commercial stainless target plate in the collision-induced dissociation (CID) MS/MS fragmentation mode. The instrument and data acquisition were controlled by TOF/TOF Explorer Software 4.1.0.

2.5.3. Data processing

Multiple spectra were analyzed using R-software (version 3.4.2) with the MALDIquant package (Gibb, 2017). Six middle spots on the MAMS chips (the first and last three spots were rejected) from each sample were analyzed, using the following steps: smoothing, baseline correction, normalization of the intensities, mass-to-charge (m/z) alignment and peak detection. Each single spectrum was smoothed using a Savitzky–Golay algorithm and the spectrum background was evaluated and corrected using the statistics-sensitive non-linear iterative peak-clipping (SNIP) algorithm. The intensities of multiple spectra were normalized using the total ion current (TIC). For comparison of peaks across different spectra, the mass values were aligned based on a warping function. The procedure involves identification of the reference peaks that occur in most spectra. Consequently, non-linear warping function is computed for each spectrum by fitting a local regression to the matched reference peaks. Features with signal-to-noise ratios (S/N) higher than 5 were detected as peaks. The identified N-glycopeptides intensities expressed as a percentage fraction relative to the sum of all glycopeptide intensities (Eq. 1).

N-Glycopeptide (%) = (*N-Glycopeptide Peak Int./Total N-Glycopeptide Int.*) x 100% (Eq. 1)

Additionally, the ratio of selected N-glycopeptides were benchmarked against the CGE-LIF method. The variability was estimated based on the following equation:

$$(Xi_{\text{FA2/FA2G1 MALDI}} - Y_{\text{FA2/FA2G1 CGE}}) / (Y_{\text{FA2/FA2G1 CGE}}) < 20\% \quad \text{(Eq. 2)}$$

where $Xi_{\text{FA2/FA2G1 MALDI}}$ denotes the intensity ratio of FA2/FA2G1 peptides for a single replicate and $Y_{\text{FA2/FA2G1 CGE}}$ the intensity ratio of FA2/FA2G1 N-glycans, respectively. The data were visualized using OriginPro 2018 software. The schematic workflow of our N-glycan pattern monitoring is presented in figure 1.

2.6. Analysis of released N-glycans

As reference analysis, the N-linked glycosylation patterns were determined using the eluates from small-scale affinity columns (Phytips®, PhyNexus, San Jose, CA) by capillary gel electrophoresis with laser-induced fluorescence detection (CGE-LIF, DNA genetic analyser, 3130 XL, Life Technologies, Darmstadt, Germany).

3. Results and discussion

3.1. MALDI-MS of N-glycopeptides

In the bottom-up approach, N-glycopeptides from complex proteolytic mixtures are often analyzed together. Therefore, the correct assignment of the *m/z* features is essential to determine the microheterogeneity of mAb glycosylation from multiple sample components. Informatics tools that facilitate MS data interpretation are certainly useful for identifying N-glycoforms. We used a web-based GlycoPepDB platform designed to facilitate compositional assignment for glycopeptides by comparing experimentally measured masses to all calculated glycopeptide masses from a carbohydrate database with N-linked glycans (Go et al., 2007). These allowed us to identify two main N-glycopeptides FA2 (*m/z* 2634) and FA2G1 (*m/z* 2796) that differ by the presence of a terminal galactose in the structure (figure 2 and table 1). Other minor forms including FA1 (*m/z* 2430), A2 (*m/z* 2487) and FA2G2 (*m/z* 2958) were also detected. Interestingly, during the time evolution of the perfusion process, we were able to recognize a rising peak with *m/z* 2405 assigned to a M5 high-mannose complex (table 1).

The N-glycoforms were additionally confirmed based on MS/MS fragmentation (figure 3) to avoid false positive matches. Different groups of fragments can be observed in the MS/MS spectrum that provide information on both peptide and attached N-glycan moieties. From these, the glycan oxonium ions, singly-protonated mono- and oligosaccharide ions, are highly sensitive markers for confident N-glycopeptide detection in CID MS/MS spectra (Wuhrer et al., 2007). In the lower mass range of the MS/MS fragment spectra (precursor ions 2430; 2487; 2634; 2796 and 2958), we identified the oxonium ions of N-acetylglucosamine (GlcNAc) at *m/z* 204 and of $Man_1GlcNAc_1$ at *m/z* 366. Moreover, the marker ions at *m/z* 186 and *m/z* 168 arising from the elimination of one or two water molecules from the GlcNAc were identified (figure 3A) (Chandler et al., 2013).

In MALDI–TOF/TOF–MS/MS, the peptide bond cleavages result predominantly in y-type and b-type fragmentation of the backbone amide bonds; with occasionally neutral losses of NH_3 or H_2O (figure 3 A). The peptide at *m/z* 1189 was determined based on different N-terminal charged fragment ions (b-type) and C-terminal charged ones (y-type) and resulted in the identification of the YNSTY amino acid sequence. Additionally, from peptide mass fingerprint (PMF) analysis of the mAb, the peptide at *m/z* 1189.5069 was assigned to the EEQYNSTYR amino acid sequence (error 4 ppm) in the constant region of IgG1. Therefore, we located the N-glycosylation site on the IgG1 Fc fragment at the Asn-Ser-Thr sequence.

Furthermore, a known fragmentation pattern of N-glycopeptides was observed in MALDI–TOF/TOF–MS/MS based on cleavages at or near the innermost N-acetylglucosamine residue, where all fragment ions retain the peptide moiety (figure 3B). We identified the prominent peak that originates from the cleavage of the side chain amide bond of the glycosylated asparagine resulting in a $[M_{pep}+H-17]^+$ ion. Moreover, peaks derived from a cross-ring fragmentation of the innercore N-acetylglucosamine with a mass of $[M_{pep} + H + 83]^+$ and from a cleavage of the chitobiose core: $[M_{pep}+H+203]^+$ (non-fucosylated core) and $[M_{pep}+H+349]^+$ (monofucosylated core) were also recognized (Wuhrer et al., 2007). All MS/MS spectra of analysed precursors confirmed the fucose residue attached to the N-acetylglucosamine, with the exception of *m/z* 2487 identified as A2 N-glycopeptide.

3.2. Micro-arrays for mass spectrometry

The signal intensities of M5, A2, FA2 and FA2G1 were presented as percentage of the total ion intensity according to the Eq. 1. Due to low signal-to-noise ratio (S/N below 3), the FA2G2 was not included in the analysis. Consequently, the coefficient of variation (CV) was calculated for each sample to express the analytical precision within a single run. The average repeatability between six spots was 1.7% and 7.1% for the FA2 and FA2G1, respectively. An example of the data distribution obtained for samples collected on day 1, 10 and 18 are presented in a boxplot in figure 4. The precision of the mean intensities from independent sample digestion did not exceeded a CV of 5% (EMA, 2011). Similar results were reported in analysis of low-molecular metabolites (Kernalléguen et al., 2018; Steinhoff et al., 2015) and monoclonal antibody in batch and perfusion cell culture (Steinhoff et al., 2016).

The analytical performance of the MAMS chip vs. deposition on a conventional stainless steel plate (384 Opti-ToF, 123 x 81 mm, AB Sciex) was evaluated by studying signal intensities of a standard FA2 glycopeptide (figure S1). Samples with concentrations from 10 pmol/µL to 10 fmol/µL were deposited onto both targets using the dried droplet method (1:1 sample-to-matrix ratio, v/v) and a total of 1000 shots per spectrum was collected with a random walk pattern. Each concentration level was measured in triplicate and for data analysis the average spectrum was calculated. Mostly, the sodium and potassium adducts as well as the protonated ions were observed. Our results show that microarray sample preparation enhanced the sensitivity and quality of mass spectra. The signal-to-noise ratios of the [M+Na]+ ions increased by 3.5 fold for the 10 and 1 pmol/µL concentrations, respectively. This proves that the µm spot size and modified surface favor consumption of the whole sample and limit the molecules from distributing unevenly on the sample spot. Consequently, the MAMS chips eliminate the time needed for searching for MALDI "hot spots" where the signal is abundant and thus support high-throughput screening and monitoring applications.

3.3. FA2 and FA2G1 monitoring

To address the applicability of MAMS, two main N-glycoforms were monitored in a time depended manner. The percentage of the FA2 ranked from 72 to 81%, whereas the FA2G1 was between 10 and 22%. For the FA2 peptide, we observed a gradual increase from day 1 to 7, followed by a rapid decrease on day 10 and 11 (figure 5A). Moreover, peaks with higher FA2 abundance were detected on days 3, 7, 9 and 13. At the same time, the percentage of the FA2G1 peptide was constantly decreasing. In total, a 2-fold decrease was observed from the start to end of the process, with the exception of outlyers on days 6, 8, 11 and 12. Both structures reached a relatively stable pattern from day 13 to the end of the bioreactor run. Considering the variation in terminal galactose abundance, two enzymes, beta-galactosidase 1 (Glb1) and beta-1,4-galactosyltransferase (B4galt1) are responsible for its removal and addition. Bertrand et al. (2019), when studying the transcriptome of CHO cells, have demonstrated B4galT1 upregulation and Glb1 downregulation at the beginning of cell cultivation. This can be correlated with the observed trend where FA2 increases and FA2 decreases over time.

Additionally, our results were compared with a routine method for glycan analysis, CGE-LIF (figure 5B, table 2). Based on the numbers in table 2 it can be concluded that the MALDI-MAMS method is favourable in terms of analysis time and shorter sample preparation. In process monitoring, a key attribute is the time needed from sampling to results being available. Therefore, fast approaches are desired to enable feedback on the running process, and to ensure continuous validation of the product. The CGE-LIF includes analysis of released N-glycans that are derivatized with a fluorophore for detection after electrophoretic separation. The ratios of the selected N-glycan structures (the same sample set) are very similar, especially for the samples collected between day 1 and 6. According to

the European Medicines Agency (EMA) guideline on bioanalytical method validation, the difference between the two values obtained from the independent methods should be within 20% of the mean for at least 67% of the repeats (EMA, 2011). We found that 83% of the FA2/FA2G1 ratios determined based on MALDI-MS agree closely with the values obtained from the reference analysis. However, samples from day 3 (CV = 22%); 9 (CV= 26%) and 13 (CV=26%) deviated.

The CGE-LIF based N-glycan analysis confirmed the FA2 structure to be the main glycoform that accounted for approximately 72 to 79% of the total glycosylation (figure S2). An increase of FA2 was observed during the first 3 days. In line with expectations, the mono-galactosylated form was detected with lower abundance. Its quantity ranged from 24 to 12% of the total oligosaccharide content, which explains the ratio fluctuations observed also in the MALDI-TOF analysis. Moreover, other forms were identified such as high mannose M5, M6 and M7, A2 and FA2G2 (figure S3). The sialylated glycans were not considered in this study, as their highest percentage amounted to only 0.3%, or they were not detected at all. Nonetheless, the reported N-glycan abundances are highly comparable to our results, with the exception of FA1 structure which was not assigned by CGF. It was demonstrated that the FA1 and M5 glycan cannot be separated by CGE-LIF (Reusch et al., 2014) and this must be taken into account in high mannose complex or afucosylation determination. When FA1 was included in the total N-glycan calculation, the abundance of the individual structure changes. Consequently, mass spectrometry as an orthogonal method has the advantage in resolving closely co-eluting compounds, and thus adding new information to glycosylation profile of mAb.

It was previously indicated (Ivarsson et al., 2014; Karst et al., 2017a) that time dependent changes of the cell environment and operating conditions affect the final product quality and glycan distribution. Particularly, the parameters such as perfusion rate and cell density have a significant impact on the CHO cells reactions (Karst et al., 2017c). The detailed behavior of CHO cells at different growth and bioreactor operating conditions were reported elsewhere (Ahn and Antoniewicz, 2011; Dean and Reddy, 2013; Goudar et al., 2010). In our study, the transient behavior of CHO cells was observed for around 6 days before reaching steady-state condition (the equilibration of reactor dynamics and cell metabolism). During the first eleven days, the process was operated at a viable cell density (VCD) of 40 x 10^6 cells/mL (figure S4), and on day 12 was increased to 50 x 10^6 cells/mL, while the perfusion rate was kept constant. As a result of the increased cell density but constant media throughput, the nutrient availability per cell decreased. The changes associated with a new VCD set point of 50x10^6 cells/mL also influenced the glycan distribution. Especially, the high mannose forms started to increase (figure S3), while the FA2G1 fraction decreased leading to a higher FA2/FA2G1 ratio as indicated in figure 5B. Similar trends have been observed based on CGE-LIF analysis by Karst et al. (Karst et al., 2017b) and were easily captured by the MAMS profiling, highlighting the potency of this method in monitoring of N-glycosylation pattern in cell culture development.

4. Conclusions

In this work, we presented a microarray-based MALDI-TOF platform as a rapid tool for N-glycan analysis during mAb production. With the aim of developing a simple analytical strategy to monitor N-glycosylation in a perfusion process, a microstructured sample carrier (MAMS) in combination with MALDI mass spectrometry was utilized. The time-dependent changes of two most abundant glycoforms FA2 and FA2G1 were used to benchmark data from MALDI MS against the established CGE-LIF method. Our results suggest that MAMS enables reproducible sample preparation with an average CV lower than 10%. The observed N-glycopeptide distributions are in agreement with data obtained from capillary gel electrophoresis, showing an increase of FA2 and a decrease of FA2G1

with manufacturing time. We therefore conclude that MAMS-based platform is very promising for glycosylation control during production of recombinant proteins.

Notes

The original data used in this publication are made available in a curated data archive at ETH Zurich (www.researchcollection.ethz.ch), DOI 10.3929/ethz-b-000324486

Acknowledgements

The authors would like to acknowledge Professor Zenon J. Kokot for helpful discussion and suggestions during the manuscript preparation. Joanna Hajduk received support from the National Science Centre in Poland within the frame of a doctoral scholarship (DEC-2015/16/T/NZ7/00033). The work has been supported by KTI (CTI)-Program (Project 19190.2 PFIW-IW).

References

Ahn, W.S., Antoniewicz, M.R., 2011. Metabolic flux analysis of CHO cells at growth and non-growth phases using isotopic tracers and mass spectrometry. Metab. Eng. 13, 598–609. https://doi.org/10.1016/J.YMBEN.2011.07.002

Barb, A.W., Prestegard, J.H., 2011. NMR analysis demonstrates immunoglobulin G N-glycans are accessible and dynamic. Nat. Chem. Biol. 7, 147–153. https://doi.org/10.1038/nchembio.511

Bertrand, V., Karst, D.J., Bachmann, A., Cantalupo, K., Soos, M., Morbidelli, M., 2019. Transcriptome and proteome analysis of steady-state in a perfusion CHO cell culture process. Biotechnol. Bioeng. 1–14. https://doi.org/10.1002/bit.26996

Callewaert, N., Contreras, R., Mitnik-Gankin, L., Carey, L., Matsudaira, P., Ehrlich, D., 2004a. Total serum proteinN-glycome profiling on a capillary electrophoresis-microfluidics platform. Electrophoresis 25, 3128–3131. https://doi.org/10.1002/elps.200406020

Callewaert, N., Vlierberghe, H. Van, Hecke, A. Van, Laroy, W., Delanghe, J., Contreras, R., 2004b. Noninvasive diagnosis of liver cirrhosis using DNA sequencer–based total serum protein glycomics. Nat. Med. 10, 429–434. https://doi.org/10.1038/nm1006

Chandler, K.B., Pompach, P., Goldman, R., Edwards, N., 2013. Exploring Site-Specific N-Glycosylation Microheterogeneity of Haptoglobin Using Glycopeptide CID Tandem Mass Spectra and Glycan Database Search. J. Proteome Res. 12, 3652–3666. https://doi.org/10.1021/pr400196s

Dean, J., Reddy, P., 2013. Metabolic analysis of antibody producing CHO cells in fed-batch production. Biotechnol. Bioeng. 110, 1735–1747. https://doi.org/10.1002/bit.24826

EMA, 2011. Guideline on bioanalytical method validation.

Fanayan, S., Hincapie, M., Hancock, W.S., 2012. Using lectins to harvest the plasma/serum glycoproteome. Electrophoresis 33, 1746–1754. https://doi.org/10.1002/elps.201100567

Gibb, S., 2017. MALDIquant: Quantitative Analysis of Mass Spectrometry Data.

Go, E.P., Rebecchi, K.R., Dalpathado, D.S., Bandu, M.L., Zhang, Y., Desaire, H., 2007. GlycoPep DB: A Tool for Glycopeptide Analysis Using a "Smart Search." Anal. Chem. 79, 1708–1713. https://doi.org/10.1021/ac061548c

Goudar, C., Biener, R., Boisart, C., Heidemann, R., Piret, J., de Graaf, A., Konstantinov, K., 2010. Metabolic flux analysis of CHO cells in perfusion culture by metabolite balancing and 2D [13C, 1H] COSY NMR spectroscopy. Metab. Eng. 12, 138–149.

https://doi.org/10.1016/J.YMBEN.2009.10.007

Hudson, P.J., Souriau, C., 2003. Engineered antibodies. Nat. Med. 9, 129–134. https://doi.org/10.1038/nm0103-129

Ivarsson, M., Villiger, T.K., Morbidelli, M., Soos, M., 2014. Evaluating the impact of cell culture process parameters on monoclonal antibody N-glycosylation. J. Biotechnol. https://doi.org/10.1016/j.jbiotec.2014.08.026

Jefferis, R., 2009. Glycosylation as a strategy to improve antibody-based therapeutics. Nat. Rev. Drug Discov. 8, 226–234. https://doi.org/10.1038/nrd2804

Karst, D.J., Scibona, E., Serra, E., Bielser, J.-M., Souquet, J., Stettler, M., Broly, H., Soos, M., Morbidelli, M., Villiger, T.K., 2017a. Modulation and modeling of monoclonal antibody N-linked glycosylation in mammalian cell perfusion reactors. Biotechnol. Bioeng. 114, 1978–1990. https://doi.org/10.1002/bit.26315

Karst, D.J., Scibona, E., Serra, E., Bielser, J.-M., Souquet, J., Stettler, M., Broly, H., Soos, M., Morbidelli, M., Villiger, T.K., 2017b. Modulation and modeling of monoclonal antibody N-linked glycosylation in mammalian cell perfusion reactors. Biotechnol. Bioeng. 114, 1978–1990. https://doi.org/10.1002/bit.26315

Karst, D.J., Serra, E., Villiger, T.K., Soos, M., Morbidelli, M., 2016. Characterization and comparison of ATF and TFF in stirred bioreactors for continuous mammalian cell culture processes. Biochem. Eng. J. 110, 17–26. https://doi.org/10.1016/J.BEJ.2016.02.003

Karst, D.J., Steinhoff, R.F., Kopp, M.R.G., Soos, M., Zenobi, R., Morbidelli, M., 2017c. Isotope labeling to determine the dynamics of metabolic response in CHO cell perfusion bioreactors using MALDI-TOF-MS. Biotechnol. Prog. 33, 1630–1639. https://doi.org/10.1002/btpr.2539

Kernalléguen, A., Steinhoff, R., Bachler, S., Dittrich, P.S., Saint-Marcoux, F., El Bakhi, S., Vorspan, F., Léonetti, G., Lafitte, D., Pélissier-Alicot, A.-L., Zenobi, R., 2018. High-Throughput Monitoring of Cocaine and Its Metabolites in Hair Using Microarrays for Mass Spectrometry and Matrix-Assisted Laser Desorption/Ionization-Tandem Mass Spectrometry. Anal. Chem. acs.analchem.7b04693. https://doi.org/10.1021/acs.analchem.7b04693

Largy, E., Cantais, F., Van Vyncht, G., Beck, A., Delobel, A., 2017. Orthogonal liquid chromatography–mass spectrometry methods for the comprehensive characterization of therapeutic glycoproteins, from released glycans to intact protein level. J. Chromatogr. A 1498, 128–146. https://doi.org/10.1016/J.CHROMA.2017.02.072

Laroy, W., Contreras, R., Callewaert, N., 2006. Glycome mapping on DNA sequencing equipment. Nat. Protoc. 1, 397–405. https://doi.org/10.1038/nprot.2006.60

Lauber, M.A., Yu, Y.-Q., Brousmiche, D.W., Hua, Z., Koza, S.M., Magnelli, P., Guthrie, E., Taron, C.H., Fountain, K.J., 2015. Rapid Preparation of Released *N* -Glycans for HILIC Analysis Using a Labeling Reagent that Facilitates Sensitive Fluorescence and ESI-MS Detection. Anal. Chem. 87, 5401–5409. https://doi.org/10.1021/acs.analchem.5b00758

Mittermayr, S., Bones, J., Doherty, M., Guttman, A., Rudd, P.M., 2011. Multiplexed Analytical Glycomics: Rapid and Confident IgG *N* -Glycan Structural Elucidation. J. Proteome Res. 10, 3820–3829. https://doi.org/10.1021/pr200371s

Nimmerjahn, F., Ravetch, J. V., 2008. Fcγ receptors as regulators of immune responses. Nat. Rev. Immunol. 8, 34–47. https://doi.org/10.1038/nri2206

Pabst, M., Altmann, F., 2011. Glycan analysis by modern instrumental methods. Proteomics 11, 631–643. https://doi.org/10.1002/pmic.201000517

Pabst, M., Fagerer, S.R., Köhling, R., Küster, S.K., Steinhoff, R., Badertscher, M., Wahl, F., Dittrich, P.S., Jefimovs, K., Zenobi, R., 2013. Self-Aliquoting Microarray Plates for Accurate Quantitative Matrix-Assisted Laser Desorption/Ionization Mass Spectrometry. Anal. Chem. 85, 9771–9776. https://doi.org/10.1021/ac4021775

Reusch, D., Haberger, M., Kailich, T., Heidenreich, A.-K., Kampe, M., Bulau, P., Wuhrer, M., 2014. High-throughput glycosylation analysis of therapeutic immunoglobulin G by capillary gel electrophoresis using a DNA analyzer. MAbs 6, 185–196. https://doi.org/10.4161/mabs.26712

Reusch, D., Tejada, M.L., 2015. Fc glycans of therapeutic antibodies as critical quality attributes. Glycobiology 25, 1325–1334. https://doi.org/10.1093/glycob/cwv065

Ruhaak, L.R., Zauner, G., Huhn, C., Bruggink, C., Deelder, A.M., Wuhrer, M., 2010. Glycan labeling strategies and their use in identification and quantification. Anal. Bioanal. Chem. 397, 3457–3481. https://doi.org/10.1007/s00216-010-3532-z

Steinhoff, R.F., Ivarsson, M., Habicher, T., Villiger, T.K., Boertz, J., Krismer, J., Fagerer, S.R., Soos, M., Morbidelli, M., Pabst, M., Zenobi, R., 2015. High-throughput nucleoside phosphate monitoring in mammalian cell fed-batch cultivation using quantitative matrix-assisted laser desorption/ionization time-of-flight mass spectrometry. Biotechnol. J. 10, 190–198. https://doi.org/10.1002/biot.201400292

Steinhoff, R.F., Karst, D.J., Steinebach, F., Kopp, M.R.G., Schmidt, G.W., Stettler, A., Krismer, J., Soos, M., Pabst, M., Hierlemann, A., Morbidelli, M., Zenobi, R., 2016. Microarray-based MALDI-TOF mass spectrometry enables monitoring of monoclonal antibody production in batch and perfusion cell cultures. Methods 104, 33–40. https://doi.org/10.1016/j.ymeth.2015.12.011

Subedi, G.P., Barb, A.W., 2015. The Structural Role of Antibody N-Glycosylation in Receptor Interactions. Structure 23, 1573–1583. https://doi.org/10.1016/j.str.2015.06.015

Villiger, T.K., Roulet, A., Périlleux, A., Stettler, M., Broly, H., Morbidelli, M., Soos, M., 2016. Controlling the time evolution of mAb N-linked glycosylation, Part I: Microbioreactor experiments. Biotechnol. Prog. 32, 1123–1134. https://doi.org/10.1002/btpr.2305

Walsh, G., 2018. Biopharmaceutical benchmarks 2018. Nat. Biotechnol. 36, 1136–1145. https://doi.org/10.1038/nbt.4305

Wong, N.S.C., Wati, L., Nissom, P.M., Feng, H.T., Lee, M.M., Yap, M.G.S., 2010. An Investigation of Intracellular Glycosylation Activities in CHO Cells : Effects of Nucleotide Sugar Precursor Feeding 107, 321–336. https://doi.org/10.1002/bit.22812

Wuhrer, M., Catalina, M.I., Deelder, A.M., Hokke, C.H., 2007. Glycoproteomics based on tandem mass spectrometry of glycopeptides. J. Chromatogr. B 849, 115–128. https://doi.org/10.1016/J.JCHROMB.2006.09.041

Zhang, L., Luo, S., Zhang, B., 2016. Glycan analysis of therapeutic glycoproteins. MAbs 8, 205–215. https://doi.org/10.1080/19420862.2015.1117719

Zhang, P., Woen, S., Wang, T., Liau, B., Zhao, S., Chen, C., Yang, Y., Song, Z., Wormald, M.R., Yu, C., Rudd, P.M., 2016. Challenges of glycosylation analysis and control: an integrated approach to producing optimal and consistent therapeutic drugs. Drug Discov. Today 21, 740–765. https://doi.org/10.1016/J.DRUDIS.2016.01.006

Table 1. Identified N-glycopeptides from the mAb sample. The observed m/z signals were searched against the GlycopepDB database with an accepted mass tolerance of 30 ppm. Abbreviations: fucose (Fuc), galactose (Gal), mannose (Man) and N-acetylglucosamine (GlcNAc).

Observed $[M+H]^+$	**Database** $[M+H]^+$	**Mass error** [ppm]	**N-glycopeptide** IgG1 mAb	**Abbrevation**
2405.9408	2405.9347	3	EEQYNSTYR-$Man_5GlcNAc_2$	M5
2430.9477	2430.9664	8	EEQYNSTYR-$GlcNAcMan_3GlcNAc_2Fuc$	FA1
2487.9542	2487.9878	14	EEQYNSTYR-$GlcNAc_2Man_3GlcNAc_2$	A2
2634.0338	2634.0457	5	EEQYNSTYR-$GlcNAc_2Man_3GlcNAc_2Fuc$	FA2
2796.0821	2796.0986	6	EEQYNSTYR-$GalGlcNAc2Man_3GlcNAc_2Fuc$	FA2G1
2958.0693	2958.1514	28	EEQYNSTYR-$Gal_2GlcNAc2Man_3GlcNAc_2Fuc$	FA2G2

Table 2. Comparison of microarray-based MALDI-TOF and CGE-LIF methods with regard to sample preparation and analytical procedure. The estimated duration of each step is included in parentheses.

Procedure steps: (± preparation time)	**MAMS-MALDI**	**CGE-LIF** (Laroy et al., 2006; Reusch et al., 2014)
mAb capture	Protein A columns (<1 h)	Protein A columns (<1 h)
In-solution enzymatic reactions	Proteolytic cleavage – trypsin (overnight inc.)	Deglycosylation - PNGase F (overnight inc.)
Fluorescent labeling	—	APTS derivatization (4 h – overnight inc.)
Sample clean-up	ZIC-HILIC chromatography (<1 h)	Size-exclusion chromatography HILIC chromatography (<1 h)
Sample/matrix deposition	MAMS technology (< 5 s per sample)	—
Detection system	MALDI-TOF (< 3 s per sample)	DNA analyzer – 96 well plate (45 min run-time for one analysis)
Peak assignment	Glycopeptide mass fingerprint MS/MS fragmentation	Alternative method (HPLC or MS) Spiking method
Total time procedure	1 day	1.5 - 2 days

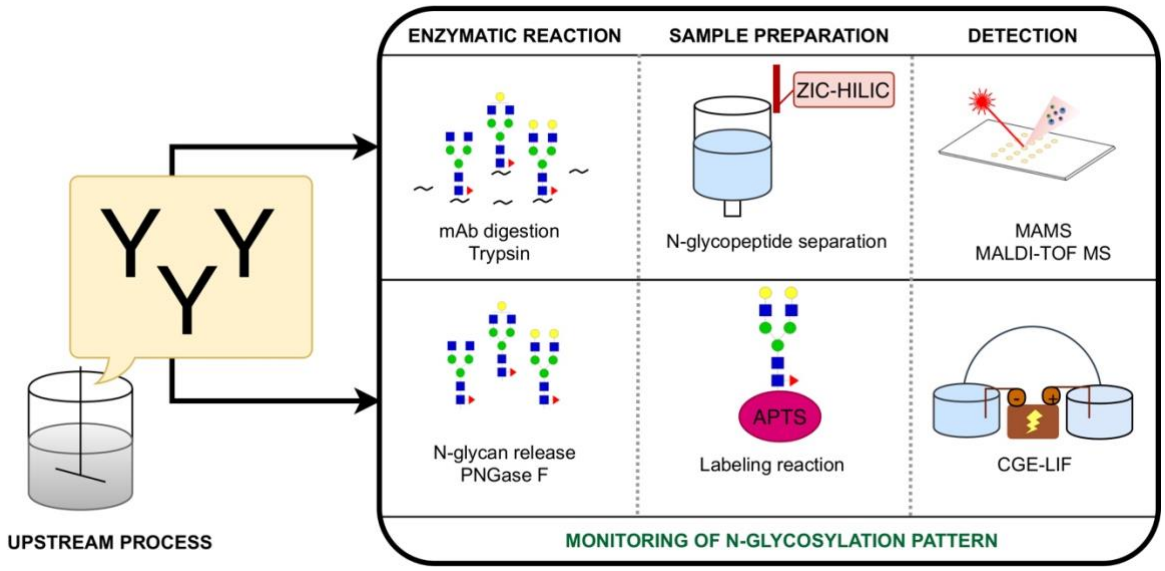

Figure 1. Schematic workflow of N-glycan analysis based on MAMS with MALDI detection and on the CGE-LIF technique.

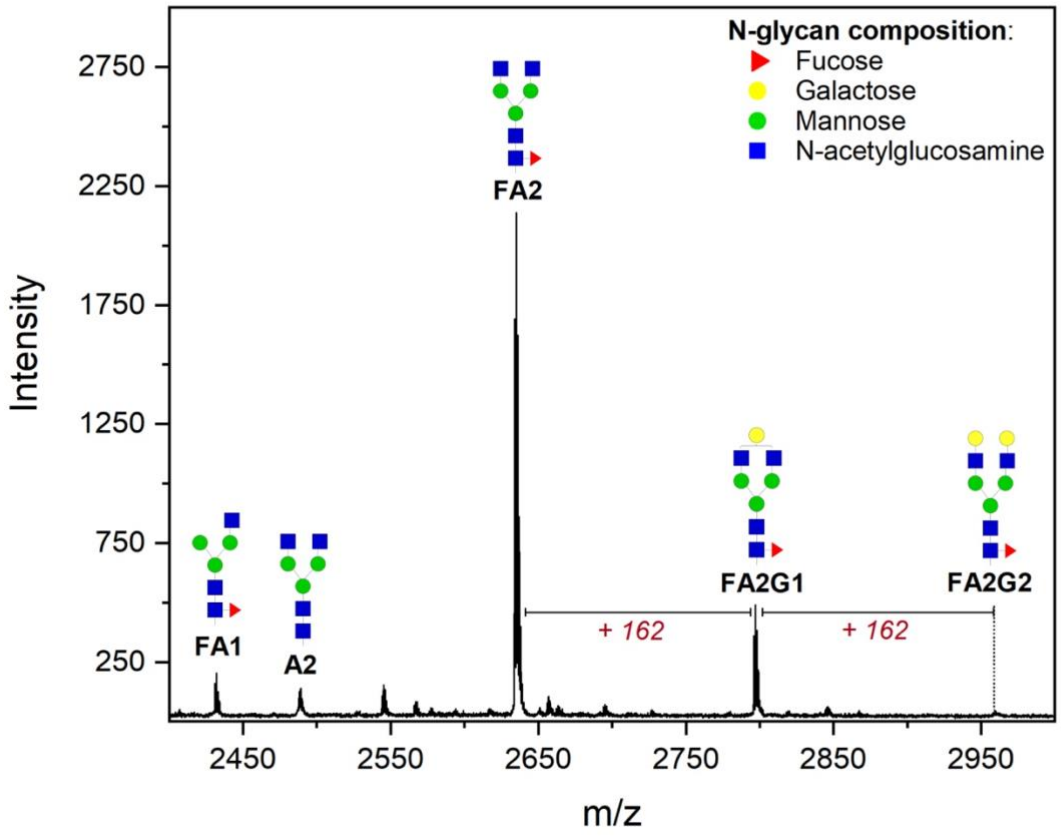

Figure 2. Representative MALDI-TOF mass spectrum of N-glycopeptides obtained from tryptic digestion of mAb (bioreactor working day 3, single MAMS spot). The two most abundant N-glycopeptides, FA2and FA2G1, which differ by a terminal galactose (±162 Da), were identified using GlycoPep DB. Other forms such as FA1, A2 and FA2G2 were also observed. N-glycan symbols: fucose (red triangles), galactose (yellow circles), mannose (green circles) and N-acetylglucosamine (blue squares).

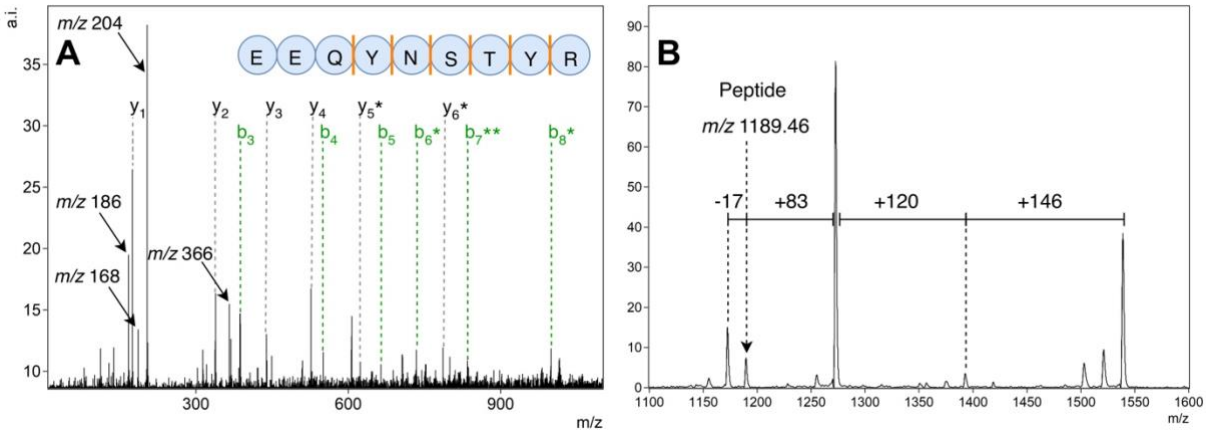

Figure 3. MALDI-TOF/TOF with CID of the tryptic N-glycopeptide from mAb. (A) Peptide sequence determined from analysis of y-type and b-type fragmentation of the backbone amide bonds with occasional deamination (asterisks) or elimination of water (double asterisks). Arrows indicate the glycopeptide marker ions in the low molecular mass range. (B) The fragmentation pattern of N-glycopeptides observed near the innermost N-acetylglucosamine with retention of the intact peptide moiety (m/z 1189.46). The prominent signal arises from the cleavage of the side-chain amide bond of the glycosylated asparagine resulting in a [Mpep+H−17]+ fragment. The following peaks derive from a cross-ring fragmentation of the innercore N-acetylglucosamine with a mass shift [Mpep+H+83]+, from a cleavage of the chitobiose core: [Mpep+H+203]+ in case of a non-fucosylated core and [Mpep+H+349]+ in case of a monofucosylated core.

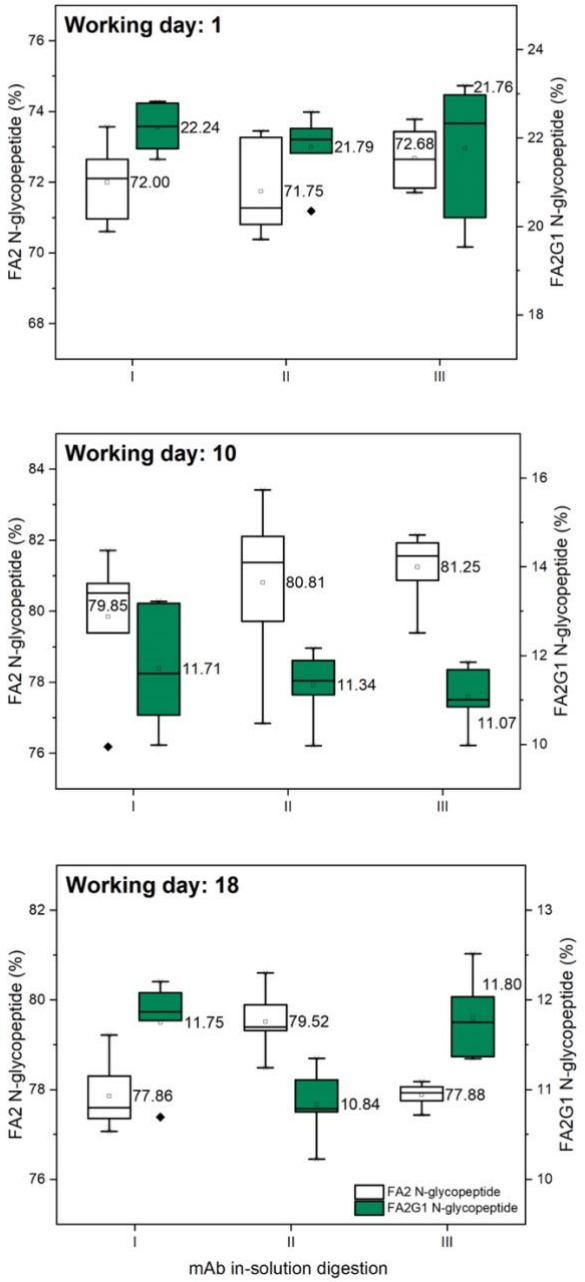

Figure 4. MAMS data distribution of FA2 and FA2G1 N-glycopeptides obtained from independent mAb digestions. The bottom and top end represent the range by the min and max observation. Within the box horizontal line indicates median, whereas the open square the mean value. The outliers are depicted by black filled diamonds. The mAb samples were collected from perfusion bioreactor on day 1, 10 and 18.

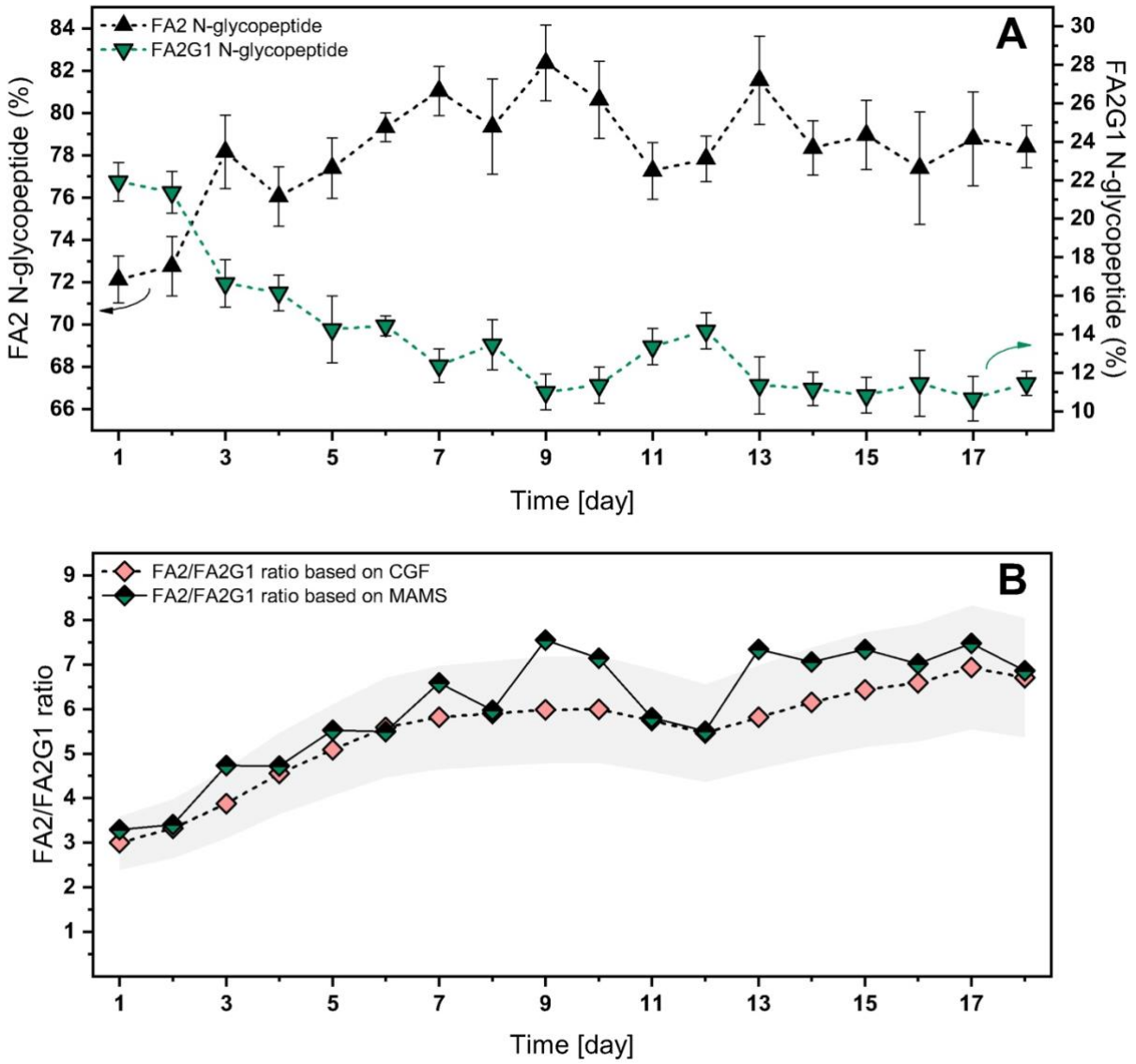

Figure 5. (A) The percentage of FA2 (black solid triangles, dotted line) and FA2G1 N-glycopeptides (green solid triangles, dotted line) determined with MALDI-TOF MS as a function of time. Each point on the graph represents the mean percentage value of triplicate sample digestion per sampling day with corresponding standard deviation. **(B)** The FA2/FA2G1 N-glycopeptide ratio (black/green diamonds, continuous line) benchmarked with FA2/FA2G1 ratio of released N-glycans (pink diamonds, dotted line) based on the CGE-LIF method. The gray area indicates mean error in cross validation of different analytical methods.